Journal of Solid State Chemistry **164,** 110–118 (2002)
doi:10.1006/jssc.2001.9454, available online at http://www.idealibrary.com on IDEAL®

The Ternary Compounds $Pd_{13}In_{5.25}Sb_{3.75}$ and $PdIn_{1.26}Sb_{0.74}$: Crystal Structure and Electronic Structure Calculations

Hans Flandorfer,[1,*] Klaus W. Richter,* Gerald Giester,† and Herbert Ipser*

*Institut für Anorganische Chemie, Universität Wien, Währingerstrasse 42, A-1090 Wien, Austria; and †Institut für Mineralogie und Kristallographie, Universität Wien, Althanstrasse 14, A-1090 Wien, Austria

Received July 23, 2001; in revised form October 8, 2001; accepted November 12, 2001

The new ternary compound $Pd_{13}In_{5.25}Sb_{3.75}$ was found. Its crystal structure was determined using a CCD diffractometer at room temperature. Evaluations and refinements finally yielded a C-centered monoclinic structure (space group, *C*2/*c*; Pearson symbol, *mC*88, $Z = 4$) with $a = 15.189(2)$ Å, $b = 8.799(1)$ Å, $c = 13.602(2)$ Å, and $\beta = 123.83(1)^\circ$. For the entire data set of 3706 independent reflections residual values are $R = 0.0461$ and $R_w = 0.0789$. The structure was found to be isotypic to $Pd_{13}Pb_9$ with In and Sb on the Pb sites. The existence of a further ternary compound, which was already described as $Pd_3In_4Sb_2$, could be confirmed. Its composition range was determined by EPMA to be $PdIn_{1.2-1.3}Sb_{0.8-0.7}$. It does not melt congruently and we were not able to find suitable single crystals. However, we were able to prepare the pure ternary compound in order to perform X-ray powder diffraction using a Guinier image plate technique. The entire diffraction spectrum was refined by full profile Rietveld method using the program Fullprof. The α-$PdSn_2$ structure type (space group, $I4_1/acd$; Pearson symbol, *t*148, $Z = 16$), proposed for this compound, was confirmed and the lattice parameters are $a = 6.4350(1)$ Å and $c = 24.3638(3)$ Å. The residual values were $R_p = 5.34$ and $R_{wp} = 6.70$. The tetragonal $PdSn_2$ structure type is a mixed variant of the CaF_2 type and the $CuAl_2$ type structure. Also in this ternary compound we assumed a random contribution of In and Sb over the 16*e* and 16*f* positions. The electronic structures of both compounds were investigated by extended Hückel calculations. Crystal orbital overlap populations show extended bonding interactions between the main group elements. The bonding interactions of the main group elements are almost optimized at the experimentally observed In/Sb ratio of the ternary compound. The In/Sb ratio in $Pd_{13}In_{5.25}Sb_{3.75}$ can thus be rationalized on the basis of the electronic structure. © 2002 Elsevier Science (USA)

Key Words: **palladium; indium; antimony; crystal structure; ternary compound; single crystal refinement; powder refinement; extended Hückel calculations.**

INTRODUCTION

Literature information concerning phase equilibria on ternary phases in the systems *T*–In–Sb (*T* = late transition metal of group 8–11) is very poor. Investigations of phase relation in the ternary phases are available for *T* = Ni (1), Cu (2, 3), Pd (4), Ag (2, 3, 5) and Au (6). However, except in (1), where a rather complete description of phase equilibria is given, just a few parts of the phase diagrams were investigated. Ternary compounds were found only in Au–In–Sb and In–Pd–Sb. For the latter system, El-Boragy and Schubert (4) reported about $Pd_3In_4Sb_2$ ($PdSn_2$-type structure, *t*48) and supposed a further ternary phase of the composition $Pd_{3.7}InSb$.

On the investigation of the system In–Pd–Sb, which was performed in the context of contact materials for III–V semiconductors, the new ternary compound $Pd_{13}In_{5.25}Sb_{3.75}$ was found and the existence of $In_4Pd_3Sb_2$ was confirmed. The latter compound is isotypic to α-$PdSn_2$ according to a recent single-crystal structure determination by Künnen *et al.* (7). Crystal structures and electronic structure calculations are reported here. Phase relations and phase diagrams will be published elsewhere (8).

EXPERIMENTAL

Sample Preparation

Samples were prepared from indium rods (99.999 mass%, ASARCO, South Plainfield, NJ), palladium sponge (99.9 mass%, ÖGUSSA, Vienna, Austria), and antimony lumps (99.99 mass%, ASARCO, South Plainfield, NJ). Calculated amounts of the pure elements were weighed to a total mass of about 2 g, sealed in evacuated quartz ampoules, and heated slowly to 1100°C for 6 h. This procedure was repeated once after powdering the sample. Samples were annealed at 850°C (14 d) and 500°C (21 d), respectively, and quenched in cold water. The total mass losses during sample preparation were less than 0.5 mass%.

EPMA

Electron microprobe analysis (EPMA) on polished samples was carried out on a Cameca SX 100 electron probe

[1]To whom correspondence should be addressed. E-mail: hans.flandorfer@univie.ac.at.

0022-4596/02 $35.00

with wavelength dispersive spectroscopy (WDS). The beam current was 20 nA at a voltage of 15 kV. For quantitative analysis In $L\alpha$, Pd $L\alpha$, and Sb $L\beta$ characteristic X-ray lines were used. Pure Pd and InSb were used as standard materials for quantitative analysis. Two ternary compounds were found in the system In–Pd–Sb within the composition range $0 \le x(\mathrm{Pd}) \le 0.6$, designated as $PdIn_{1.26}Sb_{0.74}$ and $Pd_{13}In_{5.25}Sb_{3.75}$. The homogeneity range of the first was determined by investigating samples in different two- and three-phase fields to be $Pd_{33.3}In_{40.6-43.7}Sb_{23.0-26.1}$ (corresponding to the chemical formula $PdIn_{1.2-1.3}Sb_{0.8-0.7}$). The composition of the second compound was found to be $Pd_{58.1}In_{24.5}Sb_{17.4}$; the exact homogeneity range was not determined in this case. According to changes of lattice parameters in different samples it seems to be rather small. The estimated error of quantitative analysis is $\pm$ 0.5 at.%.

Single-Crystal X-Ray Diffraction

Although it was attempted to grow single crystals of both ternary compounds this was only successful for $Pd_{13}In_{5.25}Sb_{3.75}$ whereas all structural information on $PdIn_{1.26}Sb_{0.74}$ had to be derived from its powder pattern. Single crystals of $Pd_{13}In_{5.25}Sb_{3.75}$ were picked from a crushed sample of the nominal composition $Pd_{56}In_{30}Sb_{14}$, which had been annealed at 850°C (21 d) for equilibration and crystal growth and quenched in cold water. The powder pattern (for experimental information, see below) of the sample showed the ternary compound and small amounts of two additional phases, InPd and $PdIn_xSb_{1-x}$. More details about the phase relations will be published elsewhere (8). The crystals were mounted on a glass filament and Laue photographs were obtained in order to check the crystal quality. A proper single crystal of approximate dimensions $0.04 \times 0.05 \times 0.06\ \mathrm{mm}^3$ was chosen for X-ray diffraction. Single-crystal data were collected at room temperature with a Nonius KappaCCD diffractometer (Mo$K\alpha$ radiation) equipped with a 0.3-mm capillary optics collimator. Measurement conditions were as follows: 28-mm crystal–detector distance, frames with 2° rotation width and 2×70-sec exposure time/frame. Nine sets of scans (518 frames total) were needed to complete the sphere.

The observed reflections could be indexed with a monoclinic cell of dimensions $a = 15.189(2)$ Å, $b = 8.799(1)$ Å, $c = 13.602(2)$ Å, and $\beta = 123.83(1)°$. Systematic absences of reflections left Cc and $C2/c$ as the only possible choices for the space group. Based on this information the structure solution and refinement were done using the SHELX-97 program package (9): the application of direct methods and subsequent refinement finally yielded 22 independent atomic positions in the space group Cc. However, we observed a strong correlation between atomic coordinates. Twenty positions were correlated in pairs and therefore the higher symmetry space group $C2/c$ was chosen. We transformed the atomic positions from Cc into the space group $C2/c$ ($2 \times 4a \rightarrow 8f$; $4a \rightarrow 4e$). Subsequent refinement cycles resulted in reasonable parameters and good residual values. All crystal and refinement data for $Pd_{13}In_{5.25}Sb_{3.75}$ are listed in Table 1. Atomic coordinates and equivalent isotropic displacement parameters are listed in Table 2. The full set of refinement data and anisotropic displacement factors are available from the authors (10). The Pd positions could be clearly distinguished from positions of the main group elements. In a first attempt the main group element positions were occupied by indium only in order to observe some preferences for a certain distribution of In and Sb. The isotropic displacement parameters did not indicate any preference of Sb for certain atomic positions. Several trials to refine an ordered or partially ordered distribution of In and Sb failed and we assumed totally mixed main group element positions (M = 58 at.% In + 42 at.% Sb) according to the EPMA analysis of the sample. The very similar scattering factors of In and Sb, however, make it difficult to distinguish random from ordered distributions with the X-ray diffraction technique applied. Therefore, the totally mixed occupation that is assumed here should rather be considered due to

TABLE 1
Crystal Data and Structure Refinement for $Pd_{13}In_{5.25}Sb_{3.75}$

Empirical formula	$Pd_{13}In_{5.25}Sb_{3.75}$
Formula weight	2442.82
Temperature	Room temperature
Heat treatment	850°C for 14 d, quenched in cold water
Wavelength	0.71073 Å (Mo$K\alpha$)
Crystal system	Monoclinic
Space group	$C2/c$; No. 15, unique axis b, cell choice 1
Unit cell dimensions	$a = 15.189(2)$ Å $b = 8.799(1)$ Å, $\beta = 123.83(1)°$ $c = 13.602(2)$ Å
Volume	1510.1(3) Å^3
Z	4
Density (calculated)	10.744 g/cm^3
Absorption coefficient	29.420 mm^{-1}
Crystal size	$0.04 \times 0.05 \times 0.06$ mm^3
Theta range for data collection	2.82° to 36.95°
Index ranges	$-25 \le h \le 25$, $-14 \le k \le 14$, $-22 \le l \le 22$
Reflections collected	7076
Independent reflections	3706 (R(int) = 0.0272)
Completeness to $\theta = 36.95°$	96.9%
Refinement method	Full-matrix least-squares on F^2
Data/restraints/parameters	3706/0/102
Goodness-of-fit on F^2	1.081
Final R indices [$I > 2\sigma(I)$][a]	$R1 = 0.0332$, w$R2 = 0.0733$
R indices (all data)[a]	$R1 = 0.0461$, w$R2 = 0.0789$
Extinction coefficient	0.00075(2)
Largest diff. peak and hole	3.17 and -2.65 e Å^{-3}

[a] $R = \Sigma \| F_o \| - |F_c| / \Sigma |F_o|$, $R_w = (\Sigma w(|F_o| - |F_c|)^2 / \Sigma w(F_o)^2)^{1/2}$, $w = 1/(\sigma^2 F_o^2 + (axP)^2 + (bxP))$.

TABLE 2
Atomic Coordinates and Equivalent Isotropic Displacement Parameters ($Å^2 \times 10^3$) for $In_{5.25}Pd_{13}Sb_{3.75}$[a]

Atom	Wyckoff site	x	y	z	U_{eq}
Pd(1)	8*f*	0.0188(1)	0.3874(1)	0.1272(1)	13(1)
Pd(2)	8*f*	0.0246(1)	0.1377(1)	0.6395(1)	15(1)
M(1)[b]	8*f*	0.1023(1)	0.1251(1)	0.1213(1)	12(1)
Pd(3)	8*f*	0.1220(1)	0.1215(1)	0.5001(1)	10(1)
M(2)	8*f*	0.1611(1)	0.3325(1)	0.3777(1)	12(1)
Pd(4)	8*f*	0.2498(1)	0.3751(1)	0.2488(1)	13(1)
Pd(5)	8*f*	0.2827(1)	0.1246(1)	0.1327(1)	14(1)
M(3)	8*f*	0.3352(1)	0.4129(1)	0.1141(1)	11(1)
M(4)	8*f*	0.3715(1)	0.1234(1)	0.3824(1)	11(1)
Pd(6)	8*f*	0.3787(1)	0.1339(1)	0.0042(1)	14(1)
Pd(7)	4*e*	0	0.1243(1)	$\frac{1}{4}$	13(1)
M(5)	4*e*	0	0.6194(1)	$\frac{1}{4}$	10(1)

[a] U_{eq} is defined as one-third of the trace of the orthogonalized U_{ij} tensor.
[b] M = 58 at.% In + 42 at.% Sb.

the experimental limitations of the X-ray method than a proven fact; however, see the atomic orbital population analysis.

A careful comparison of the structure with structure types already described in the literature (11) revealed a similarity with the $Pd_{13}Pb_9$ structure type which was originally described in (12). After transformation of the $Pd_{13}Pb_9$ structure to a standard setting using STRUCTURE TIDY (13) $Pd_{13}In_{5.25}Sb_{3.75}$ was found to be a ternary variant of the $Pd_{13}Pb_9$ structure type, with the Pb atoms substituted by a mixture of In and Sb.

X-Ray Powder Diffraction

All powder patterns were obtained with a Guinier-Huber film chamber using Cu$K\alpha_1$ radiation and employing an internal standard of high-purity Si. In order to determine the crystal structure of $PdIn_{1.26}Sb_{0.74}$ various samples were prepared around $Pd_3In_4Sb_2$, as reported in (4), and annealed at 500°C (21 d). In all cases the powder patterns showed the ternary compound as an equilibrium phase which could be indexed on the basis of the structural description given in (4). In the same samples, however, annealed at 700°C (14 d), the ternary compound disappeared. Therefore, the ternary phase melts incongruently.

The lattice parameters varied slightly but significantly in agreement with the small homogeneity range evaluated by EPMA (see above), and the observed intensities were in good agreement with those given by El-Boragy and Schubert (4). These authors concluded that the structure was isotypic to tetragonal $PdSn_2$ (14) by direct comparison of the intensities. However, intensity patterns given in (4) for $Pd_3In_4Sb_2$ and in (14) for α-$PdSn_2$ both did not agree with the intensities calculated here, based on crystallographic information given in (14). Calculated intensities based on a recent single-crystal refinement by Künnen *et al.* (7) for α-$PdSn_2$ were in excellent agreement with our powder pattern of $PdIn_{1.26}Sb_{0.74}$. To confirm isotypism of the two compounds it was decided to refine the crystal structure of $PdIn_{1.26}Sb_{0.74}$.

As various attempts to find proper single crystals failed, a sample of the composition $Pd_{33}In_{42}Sb_{25}$ was annealed at 500°C (21 d) in order to obtain the pure ternary compound for refinement of the powder diffraction pattern. A Guinier-Huber G670 image plate system with Cu $K\alpha_1$ radiation was used to record the powder pattern. Rietveld refinement of this pattern was carried out using the program FULLPROF (15). Based on a crystallographic data set derived from the $CoGe_2$-type structure by doubling the *c*-axes as described in (14) we obtained reasonable results and satisfying residual values. Refinement details and lattice parameters for the compound $PdIn_{1.26}Sb_{0.74}$ are listed in Table 3. Atomic coordinates and isotropic temperature factors are presented in Table 4. For the same reasons we described above for $Pd_{13}In_{5.25}Sb_{3.75}$, a mixed occupation of the main group element positions by In and Sb had to be assumed.

Extended Hückel Calculations

Extended Hückel calculations were performed using the Caesar program package (16). As it is not possible to handle

TABLE 3
Crystal Data and Structure Refinement for $PdIn_{1.26}Sb_{0.74}$

Empirical formula	$PdIn_{1.26}Sb_{0.74}$
Formula weight	341.60
Temperature	Room temperature
Heat treatment	500°C for 21 d, quenched in cold water
Wavelength	1.54056 Å (Cu$K\alpha$1)
Crystal system	Tetragonal
Space group	$I4_1/acd$; No. 142, cell choice 2
Unit cell dimensions	a = 6.4350(1) Å c = 24.3638(3) Å,
Volume	1008.88(4) $Å^3$
Z	16
Density (calculated)	8.995 g/cm^3
2 Theta range for data collection	18.00° to 100.00°
Step size in 2θ	0.005
Independent reflections	133
Refinement method	Full-matrix full-profile powder data refinement
Final profile R indices[a]	R_p = 5.34, R_{wp} = 6.70
Bragg R-factor[b]	R_B = 5.79
F R-factor[c]	R_F = 5.12

[a] $R_p = 100 \times \Sigma|y_{oi} - y_{ci}|/\Sigma|y_{oi}|$, $R_{wp} = 100 \times (\Sigma w_i|y_{oi} - y_{ci}|^2/\Sigma w_i|y_{oi}|^2)^{1/2}$, $w_i = 1/\text{variance(obs)}i$; background uncorrected.
[b] $R_B = 100 \times \Sigma|I_o - I_c|/\Sigma|I_o|$, I = integrated intensity.
[c] $R_F = 100 \times \Sigma||F_o| - |F_c||/\Sigma|F_o|$.

TABLE 4
Atomic Coordinates ($\times 10^4$) and Isotropic Temperature Parameters for $In_{1.26}PdSb_{0.74}$[a]

Atom	Wyckoff site	x	y	z	B (Å^2)
$M(1)$[b]	16*f*	0.1598(1)	0.4098(1)	$\frac{1}{8}$	2.60(2)
$M(2)$	16*e*	0.2494(1)	0	$\frac{1}{4}$	2.20(2)
Pd(1)	16*d*	0	$\frac{1}{4}$	0.31619(2)	2.24(2)

[a] U_{eq} is defined as one-third of the trace of the orthogonalized U_{ij} tensor.
[b] M = 63 at.% In + 37 at.% Sb.

mixed site occupancies within the extended Hückel approximation, the calculations were performed on hypothetical binary Pd–In compounds. The structural parameters obtained by the structure refinements of the respective ternary compounds were used and the Fermi levels were adapted according to the empirical ternary composition. The Hückel parameters used for the calculations are listed in Table 5. Parameters for In were taken from standard sources (16) while the parameters for Pd were obtained by solid-state charge iteration on binary Pd_5In_3 (Ge_3Rh_5-type, *oP*16).

RESULTS AND DISCUSSION

$Pd_{13}In_{5.25}Sb_{3.75}$

The ternary phase of the composition $Pd_{3.7}InSb$ which was reported in (4) (compare Introduction) was claimed to be a solid solution of In in Pd_5Sb_3, which crystallizes in a filled NiAs-type structure (17). The corresponding X-ray powder patter, however, could not be indexed on the basis of the binary structure type by the authors, and therefore a superstructure was supposed (4). Although the Pd content of the phase $Pd_{13}In_{5.25}Sb_{3.75}$ identified here is significantly different from that of $Pd_{3.7}InSb$ (59 at.% compared to 65 at.%) it is still possible that these two phases are identical since the composition $Pd_{3.7}InSb$ had only been estimated by El-Boragy and Schubert (4). However, the structure of $Pd_{13}In_{5.25}Sb_{3.75}$ clearly shows that it is a true ternary phase rather than a solid solution of In in binary Pd_5Sb_3.

The compound $Pd_{13}In_{5.25}Sb_{3.75}$ crystallizes in the monoclinic structure type $Pd_{13}Pb_9$. This structure type can be considered as a distorted and partly filled member of the NiAs family. The hexagonal unit cell of NiAs or of its completely filled variant Ni_2In may be regarded as a principal building block of the monoclinic structure type $Pd_{13}Pb_9$. Four of these building blocks, stacked in the (0 0 1) plane, yield a new hexagonal subunit with doubled *a*- and *b*- axes. An orthorhombic setting of this new hexagonal subunit and stacking of four such orthorhombic units along (0 0 1) give a new orthorhombic cell with $a_o = a_h\sqrt{3}$; $b_o = b_h$; $c_o = 4c_h$. This orthorhombic cell can be considered as the pseudoorthorhombic setting of the monoclinic cell of $Pd_{13}In_{5.25}Sb_{3.75}$ (see Fig. 1). Lattice parameters of the two cells are related according to $a_o = a_m$, $b_o = b_m$, and $c_o = 2c_m \sin(180^\circ - \beta_m)$. The condition for a pseudoorthorhombic geometry of a monoclinic unit cell is $a = 2c \cos(180^\circ - \beta)$. For $Pd_{13}In_{5.25}Sb_{3.75}$ $a = 15.189(2)$ Å, $b = 8.799(1)$ Å, $c = 13.602(2)$ Å, and $\beta = 123.83(1)^\circ$, revealing small but significant deviations from the ideal axes relations described above corresponding to a small distortion of the cell metric from the ideal one constructed with hexagonal subunits.

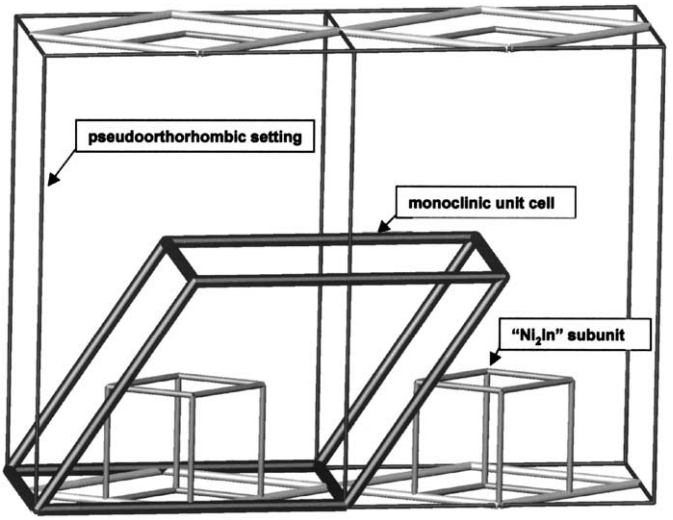

FIG. 1. Geometrical relationship between the monoclinic cell of the $Pd_{13}Pb_9$ structure type, the hexagonal "Ni_2In-type" (or "NiAs-type") subunit, and the pseudoorthorhombic setting.

Figure 2 shows a projection of the unit cell on the (0 0 1) plane. The dashed lines indicate the (0 0 1) plane of a pseudohexagonal "Ni_2In" building block. Figure 3 shows a perspective view perpendicular to the (0 0 1) plane. From this perspective the structure appears to be built up of two different kinds of atom columns. The first kind, corresponding to the 2*a* Ni sites in the Ni_2In structure type, is essentially straight and consists of seven Pd positions and one *M* position. The second kind of columns is not straight and consists of alternating Pd and *M* positions. However, one-fourth of the Pd positions are not occupied and form vacancies that are separated by seven atoms, four *M* and three

TABLE 5
Parameters Used in the Extended Hückel Calculations

Orbital	H_{II}/eV	ζ_1	c_1	ζ_2	c_2
Pd, 5*s*	− 6.11	2.19			
Pd, 5*p*	− 2.82	2.15			
Pd, 4*d*	− 10.34	5.98	0.553	2.61	0.670
In, 5*s*	− 12.60	1.90			
In, 5*p*	− 6.19	1.68			

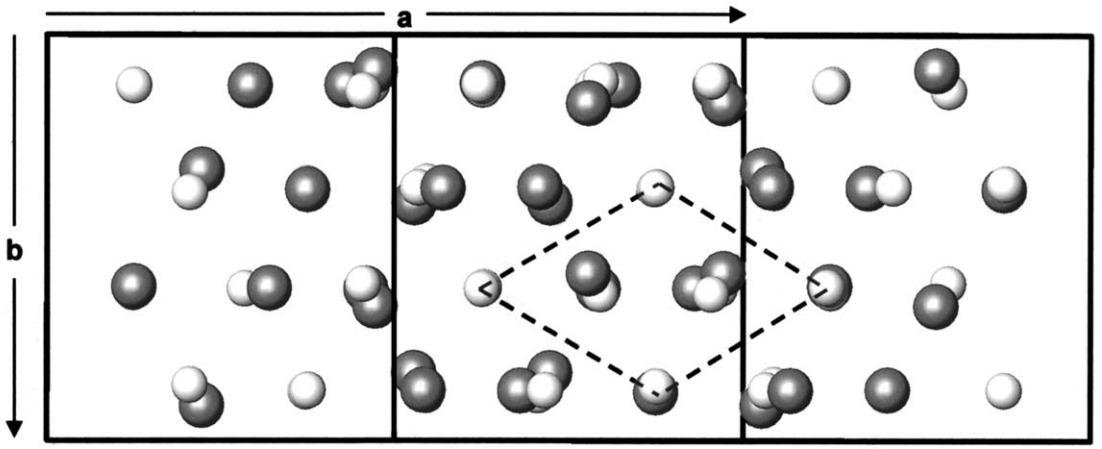

FIG. 2. Projection of the unit cell of $Pd_{13}In_{5.25}Sb_{3.75}$ on the (0 0 1) plane. The dashed line indicates the hexagonal subunit. Bright atoms, Pd; dark atoms, *M* (In, Sb).

Pd atoms. Neighboring main group atoms in the (0 0 1) plane move onto the vacancies and reduce their interatomic distances to about 75%. In contrast, the *M*–*M* distances along the atom columns are essentially not influenced by the vacancies.

A complete list of interatomic distances up to 3.5 Å can be obtained from the authors (10). The shortest distances are 2.656 Å for Pd(1)–*M*(1), 2.792 Å for Pd(2)–Pd(6), and 3.235 Å for *M*(2)–*M*(2). Figure 4 shows the coordination spheres of three different main group element positions, *M*(1), *M*(2), and *M*(5), up to 3.5 Å. Essential "bonds" are indicated between *M* atoms (thick line) and between *M* and Pd atoms (thin line). Figure 4a shows the coordination of *M*(1) which is situated within the second sort of columns. There are only Pd atoms in the coordination sphere. Three of them have the shortest Pd–*M* distances (below 2.7 Å, drawn as *M*–Pd bonds) occurring in this structure. The distorted prism formed by six further Pd atoms is indicated with black tie lines. One more Pd atom is situated above the prism with a *M*(1)–Pd distance of 2.949 Å. The coordination sphere of *M*(2), which is situated adjacent to a Pd vacancy, is shown in Fig. 4b. *M*(2) is surrounded by two *M* positions, *M*(2) and *M*(5), and eight Pd atoms. The rather short *M*(2)–*M*(2) distance is caused by the shift of main group positions onto the vacancies (see above). The distorted prism, indicated with black tie lines, is formed by five Pd atoms and one main group element at *M*(5). The atomic position *M*(5) corresponds to be the main group elements (2*a* site in the hypothetical $InNi_2$ subunit). Its coordination sphere is shown in Fig. 4c. Eight Pd atoms and six main group elements, two *M*(2), two *M*(3), and two *M*(4), are coordinated with rather short distances of less than 3.35 Å. Bonds to Pd atoms in the straight columns are colored black.

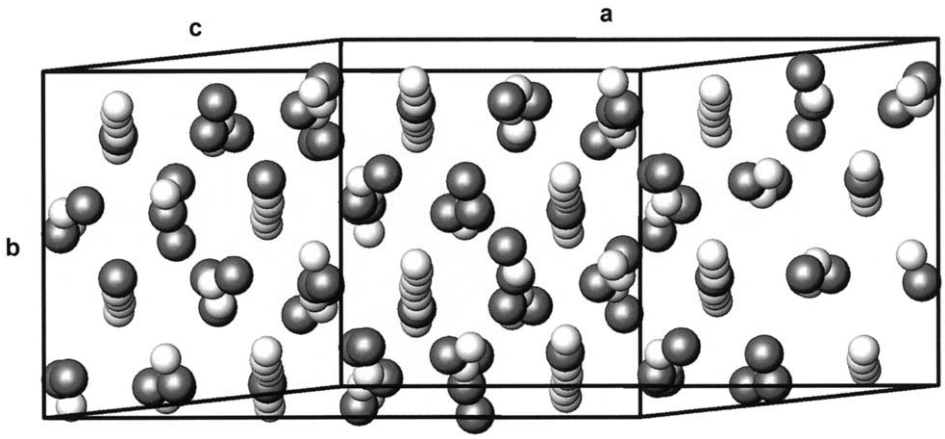

FIG. 3. Perspective view of $Pd_{13}In_{5.25}Sb_{3.75}$ perpendicular to the (0 0 1) plane showing different types of atom columns with the unit cell indicated. Bright atoms, Pd; dark atoms, *M* (In, Sb).

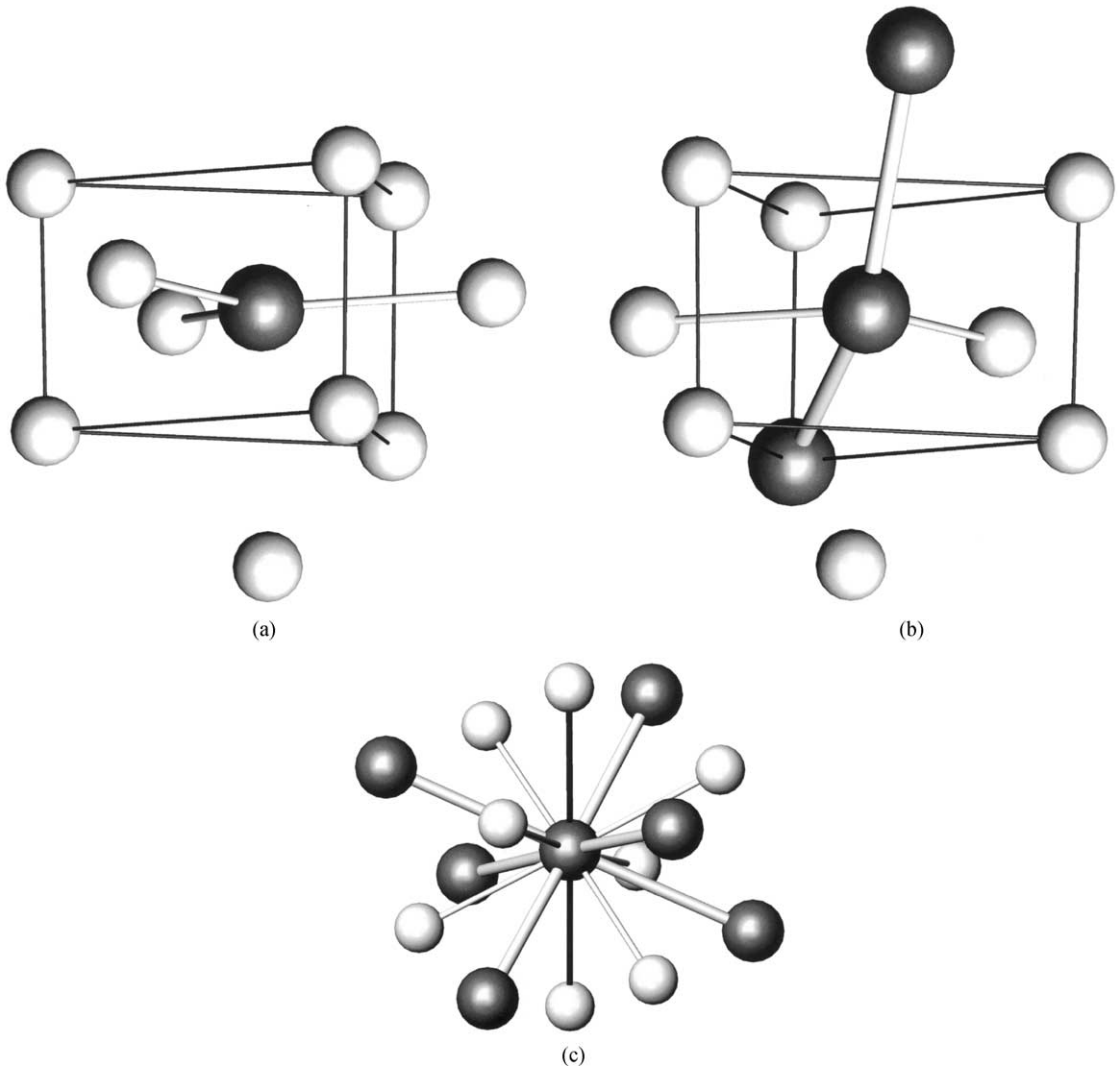

FIG. 4. Coordination spheres of selected main group element positions: (a) *M*(1), (b) *M*(2), and (c) *M*(5). Bright atoms, Pd; dark atoms, *M* (In, Sb).

Electronic structure calculations using the extended Hückel approach were performed in order to gain deeper insight into chemical bonding in $Pd_{13}In_{5.25}Sb_{3.75}$. The calculation was performed on hypothetical binary $Pd_{13}In_9$ using the structural parameters in Table 2. The density of states (DOS) curve for $Pd_{13}In_{5.25}Sb_{3.75}$ is shown in Fig. 5a. The very high density of states at approximately -10 eV corresponds almost entirely to the Pd *d*-states. For a better representation of the other parts of the DOS curve this peak is not shown completely. The peak occurs at energies around the Pd 4*d* orbital energies (compare Table 5), which indicates that these orbitals do not play an important role in the stabilization of this compound. The Fermi level at -6.52 eV corresponds to the empirical composition of $Pd_{13}In_{5.25}Sb_{3.75}$ (658 electrons per unit cell). The states situated around the Fermi level show Pd 5*p* as well as In 5*s* and 5*p* contributions. The Mulliken overlap population (MOP) curves shown in Fig. 5b reveal interesting details regarding the chemical bonding in $Pd_{13}In_{5.25}Sb_{3.75}$. While the overlap population of Pd–Pd is essentially negligible around the Fermi level, In–Pd overlaps show large positive (i.e., bonding) contributions above as well as below the Fermi level indicating strong bonding interactions between In and Pd. It is interesting that there are also considerable bonding In–In contributions. In–In interactions are almost "optimized;" i.e., the transition between positive (bonding) overlaps and negative (antibonding) overlaps occurs only slightly above the Fermi level of the ternary compound $Pd_{13}In_{5.25}Sb_{3.75}$. The optimization of *M*–*M* bonding may thus play some role in the composition (i.e., x_{In}/x_{Sb} ratio) actually adopted in the ternary compound $Pd_{13}In_{5.25}Sb_{3.75}$. Fermi levels of the hypothetical binary compounds $Pd_{13}In_9$ (628 electrons/unit cell; $E_F = -7.42$ eV) and $Pd_{13}Sb_9$ (700 electrons/unit cell; $E_F = -4.80$ eV) are shown

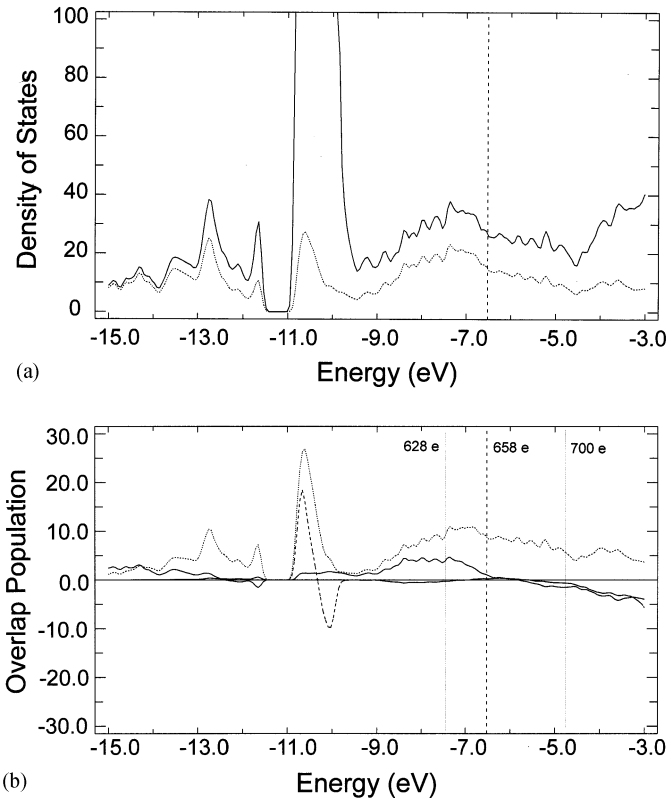

FIG. 5. (a) Density of states (DOS) of hypothetical binary "$Pd_{13}In_9$." Solid line: overall DOS. Dotted line: In contribution. Fermi level corresponding to $Pd_{13}In_{5.25}Sb_{3.75}$ (658 electrons per unit cell). (b) Mulliken overlap populations for $Pd_{13}In_9$. Solid line: In–In contribution. Dashed line: Pd–Pd contribution. Dotted line: In–Pd contribution. Fermi levels shown for 628, 658, and 700 electrons per unit cell, respectively.

in Fig. 5 together with the Fermi level for $Pd_{13}In_{5.25}Sb_{3.75}$. A more detailed investigation of the crystal orbital overlap populations reveals that a large part of the overlap population count for In–In is due to a few relatively short *M*–*M* contacts. These "bonds" are the contacts between *M*(5)–*M*(2) (0.31 electron/bond), *M*(5)–*M*(3) (0.27 electron/bond), *M*(5)–*M*(4) (0.29 electron/bond) which all involve the main group atom at the position *M*(5) within the linear column (Fig. 4c) and the short contacts *M*(2)–*M*(2) (0.30 electron/bond) shown in Fig. 4b. One may thus conclude that the "odd" *M*5 position within the straight Pd atom columns as well as the Pd vacancies that promote the formation of short *M*2–*M*2 contacts essentially contribute to the considerable amount of *M*–*M* overlap observed in this special structure type.

The tool of atomic orbital population analysis has been successfully used to investigate "coloring" problems in solid state chemistry (18). According to this approach, it is possible to investigate possible site preferences among closely related elements within a structure by analyzing the atomic orbital populations of different sites. If different atomic sites exhibit large differences in atomic orbital population, one may predict that the more electronegative element will preferably occupy the sites with the higher atomic orbital population. As we were not able to distinguish between In and Sb positions in the case of the compound $Pd_{13}In_{5.25}Sb_{3.75}$ on the basis of X-ray diffraction data (compare previous section), we decided to use atomic orbital population analysis to investigate this problem. The atomic orbital populations obtained for the five different *M* positions $Pd_{13}In_{5.25}Sb_{3.75}$, however, were found to exhibit rather small differences (3.10–3.23 electrons/atom) and thus do not point toward distinct site preferences among In and Sb.

$PdIn_{1.26}Sb_{0.74}$

In a recent single-crystal refinement of the tetragonal $PdSn_2$-type structure by Künnen *et al.* (7) agreement with the structure determination reported earlier for the same compound by Hellner (14) was stated. Our results of crystal structure refinement of isotypic $PdIn_{1.26}Sb_{0.74}$ are in excellent agreement with those of Künnen *et al.* (7) but not those of Hellner (14), who reported a different *z*-parameter at the 16*d* position. At first glance, the observed difference of 0.04 appears to be relatively small. However, considering the long *c*-axes and the symmetry of the 16*d* position, interatomic distances were significantly changed (up to ~ 1.6 Å, for Pd–Pd), leading to extended changes in the respective coordination spheres. Furthermore, it should be noted that likewise the intensities given for α-$PdSn_2$ (14) do not fit to the calculated pattern based on structural information given in this paper and that the coordination figures and interatomic distances calculated with these values (11) are rather unrealistic; e.g., there are the shortest Pd–Sn distances of 2.431 Å, which is 10% below the sum of the covalent Pauling radii. We therefore conclude that the *z*-parameter for the 16*d* position of this structure type originally reported by Hellner (14) is inaccurate and the structure determination for α-$PdSn_2$ reported by Künnen *et al.* (7) is the correct model for this structure type. There the *z*-parameter of the 16*d* position of α-$PdSn_2$ is 0.31671(3) and differs by only 0.00052 from that of $PdIn_{1.26}Sb_{0.74}$ (see Table 3).

The α-$PdSn_2$ structure type belongs to a family which is called "mixed CaF_2-type structures". They are built up from atomic layers of the CaF_2 type mixed with layers from other structure types. One group of this family includes combinations of the CaF_2 type with the $CuAl_2$-type structure. The $CoGe_2$-type, the $RhSn_2$-type, and finally the tetragonal $PdSn_2$-type structures belong to this group. For more details see Refs. (7, 13).

The shortest interatomic distances in $PdIn_{1.26}Sb_{0.74}$ are 2.865 Å for Pd–Pd, 2.787 Å for Pd–*M*, and 2.909 Å for *M*–*M*, where *M* designates the main group element positions with mixed occupation (63 at.% In + 37 at.% Sb); see

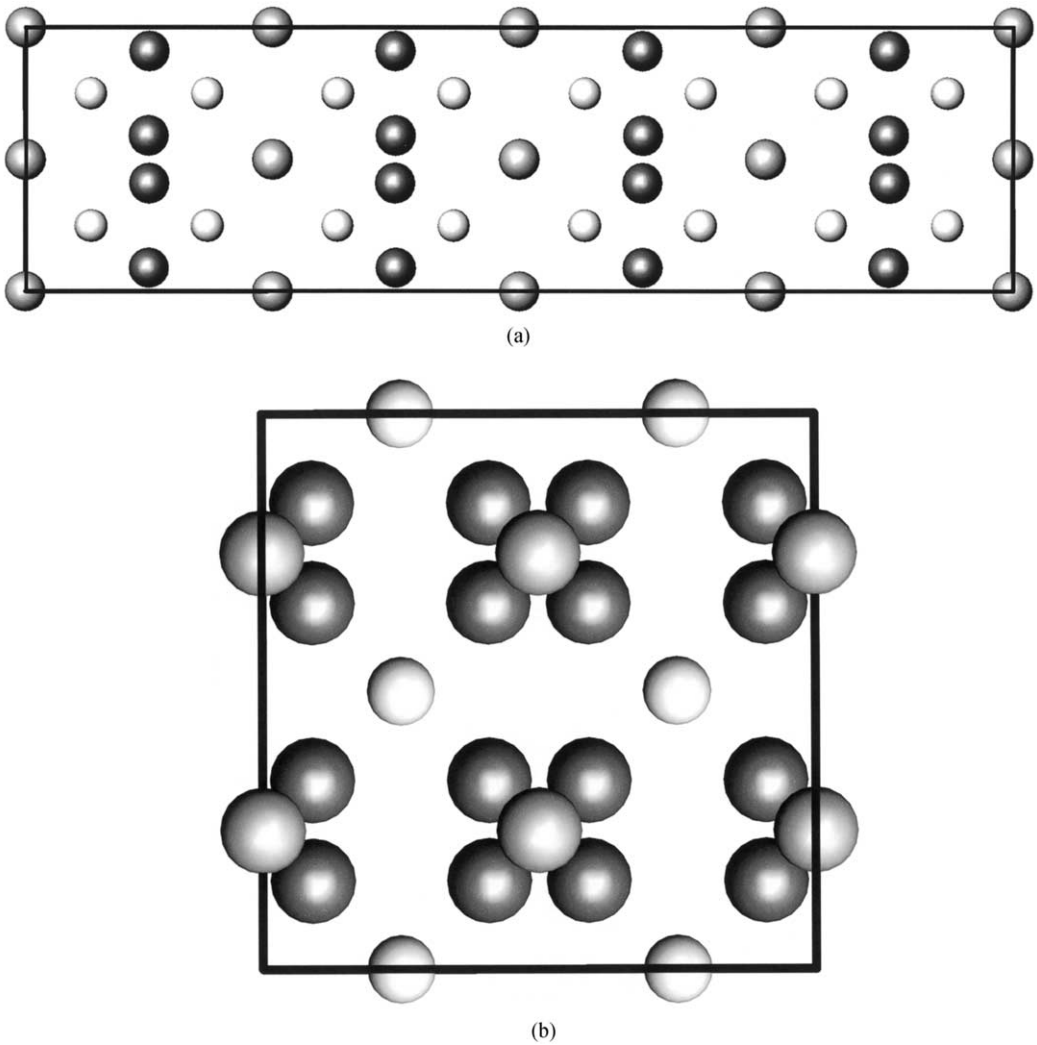

FIG. 6. Two different projections of the unit cell of $PdIn_{1.26}Sb_{0.74}$: (a) projection along (1 0 0); (b) projection along (0 0 1). Bright atoms, Pd; gray atoms; $M(1)$; dark gray atoms, $M(2)$.

also Table 4. This is in good agreement with the atomic radii of the elements. A complete list of interatomic distances up to 4.0 Å is available from the authors (10).

In Fig. 6 two different projections of the unit cell are presented. Figure 6a is a projection along (1 0 0) and Fig. 6b along (0 0 1). Figure 7 shows a perspective view along (0 0 1). The Pd atoms (at 16*d*; see also Table 4) are arranged in pairs with a distance of 2.865 Å. These pairs form straight and unmixed columns along (0 0 1) with the long distance of 9.317 Å between the pairs. The main group elements at the 16*e* position form almost straight and unmixed atom columns with an interatomic distance of 6.091 Å. The main group elements at the 16*f* position are helix-like wound around the straight rows of main group elements. The interatomic distances amount to 6.201 Å.

In order to test for possible site preferences among In and Sb, atomic orbital populations obtained by extended Hückel calculations on hypothetical binary $PdIn_2$ using the structural data for $PdIn_{1.26}Sb_{0.74}$ were analyzed. Atomic orbital populations were found to be exactly the same (3.22 electrons/atom) for both positions, $M(1)$ and $M(2)$, giving rise to the conclusion that no site preferences occur in this compound.

CONCLUSIONS

In the Pd-poor region of the Pd–In–Sb system, $0 \leq x_{Pd} \leq 0.6$, we found two ternary intermetallic compounds. One compound melts incongruently and has the composition range $PdIn_{1.2-1.3}Sb_{0.8-0.7}$. It crystallizes in the α-$PdSn_2$ structure type. The second compound, $Pd_{13}In_{5.25}Sb_{3.75}$, crystallizes in the monoclinic $Pd_{13}Pb_9$ structure type. Its melting behavior and exact homogeneity range have not yet been determined.

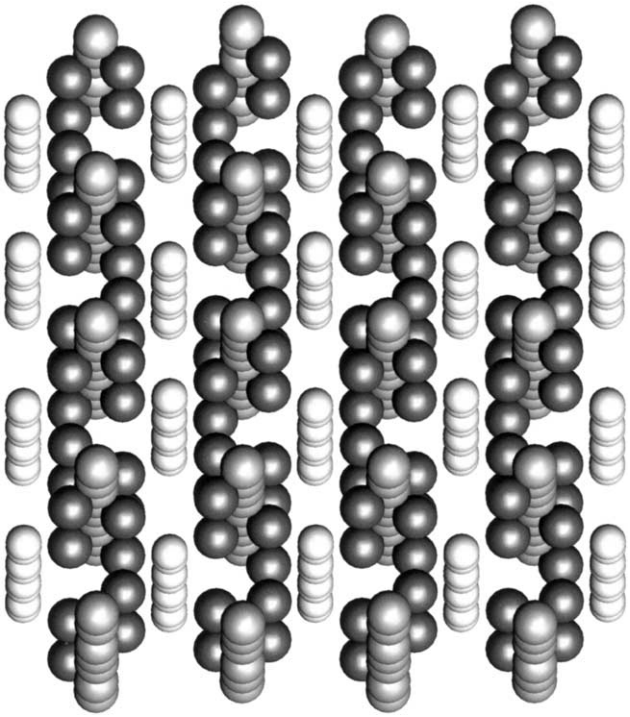

FIG. 7. Perspective view along (0 0 1) in $PdIn_{1.26}Sb_{0.74}$. White atoms, Pd; gray atoms, $M(1)$; dark gray atoms, $M(2)$

Thus both compounds crystallize in a binary structure type containing Pd. The elements Pb and Sn, respectively, with four valence electrons are substituted by a mixture of In with three and Sb with five valence electrons. The variability of the mixing ratio is rather small. Strong electronic effects and presumably as well size effects are important for the stabilization of the ternary compounds.

ACKNOWLEDGMENTS

The authors thank the FWF (Austrian Science Foundation) for financial support of this research under project No. P 10739-CHE.

REFERENCES

1. K. W. Richter, K. Micke, and H. Ipser, *Mater. Sci. Eng. B* **55,** 44 (1998).
2. G. M. Kuznetsov and A. P. Bobrov, *Izv. Vyssh. Ucheb. Zaved., Tsvet. Met.* **12,** 126 (1969).
3. G. M. Kuznetsov and A. P. Bobrov, *Inorg. Mater., Trans. Izv. Akad. Nauk SSSR, Neorg. Mater.* **7**(5), 666 (1971).
4. M. El-Boragy and K. Schubert, *Z. Metallkd.* **62,** 667 (1971).
5. G. F. Gubskaya, W. Ping-nan, N. P. Luzhnaya, and D. L. Kudryavtsev, *Inorg. Mater., Trans. Izv. Akad. Nauk SSSR, Neorg. Mater.* **1,** 188 (1965).
6. A. Prince, G. V. Raynor, and D. S. Evans, "Phase Diagrams of Ternary Gold Alloys," p. 295. The Institute of Metals, London, GB, 1990.
7. B. Künnen, D. Niepmann, and W. Jeitschko, *J. Alloys Compd.* **309,** 1 (2000).
8. C. Luef, H. Flandorfer, K. Richter, and H. Ipser, in preparation.
9. G. M. Sheldrick, SHELX-97, University of Göttingen, Germany, 1997.
10. http://www.ap.univie.ac.at/users/Klaus.Richter/publ.html.
11. J. L. C. Daams, P. Villars, and J. H. N. van Vucht, "Atlas of Crystal Structure Types for Intermetallic Phases." ASM International, Materials Park, OH, 1991.
12. H. W. Mayer, M. Ellner, and K. Schubert, *J. Less-Common Met.* **71,** P29–P38 (1980).
13. L. M. Gelato and E. Parthe, *J. Appl. Crystallogr.* **20,** 139 (1987).
14. E. Hellner, *Z. Kristallogr.* **107,** 99 (1956).
15. J. Rodriguez-Carvajal, "FULLPROF Version 3.1c." Lab. Leon Brillouin, France, 1996.
16. J. Ren, W. Liang, and M. H. Whangbo, "CAESAR Software." North Carolina State University, NC, 1998.
17. K. Schubert, K. Anderko, M. Kulge, H. Beeskow, M. Ilschner, E. Dorre, and P. Esslinger, *Naturwissenschaften* **40**(9), 269 (1953).
18. G. J. Miller, *Eur. J. Inorg. Chem.* **5,** 523 (1998).